Supplementary Materials: Slow Magnetic Relaxation in Unprecedented Mono-Dimensional Coordination Polymer of Ytterbium Involving Tetrathiafulvalene-Dicarboxylate Linker

Anjara Belio Castro, Julie Jung, Stéphane Golhen, Boris Le Guennic, Lahcène Ouahab, Olivier Cador, Fabrice Pointillart

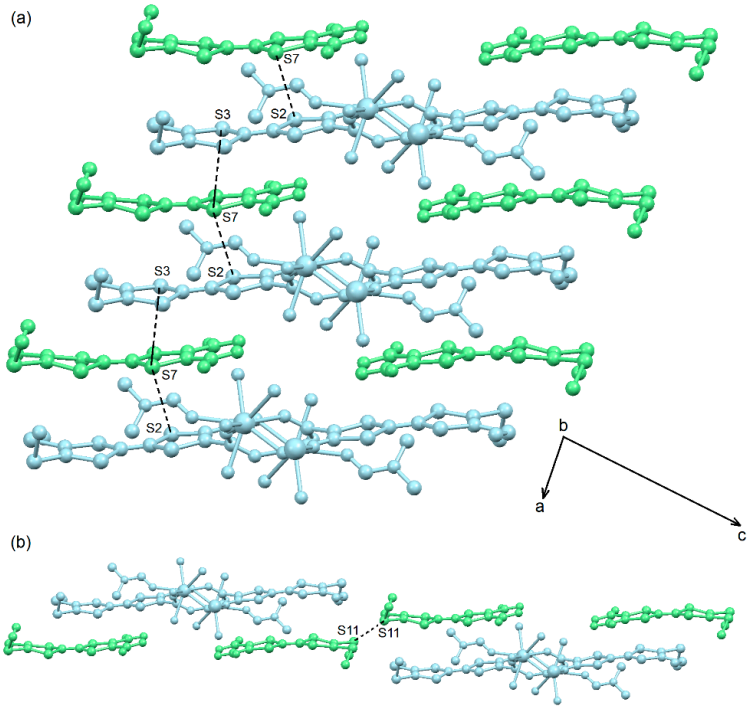

Figure S1. (**a**) Crystal packing of **Yb** highlighting the interactions with the **HL**$^-$ counter anions through the S···S short contacts; (**b**) Representation of the S···S short contacts between the **HL**$^-$ mono-anions.

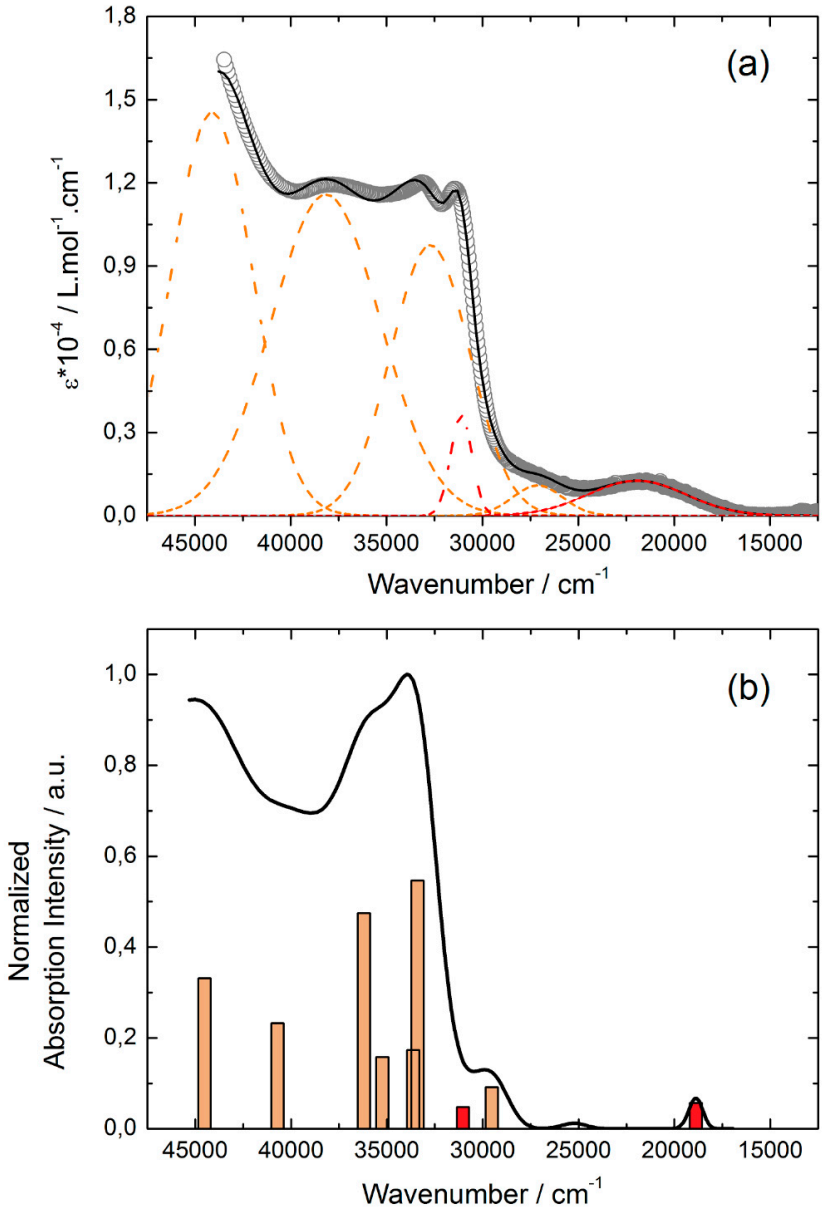

Figure S2. (**a**) Experimental UV-VIS absorption spectra in CH_2Cl_2 solution of **H_2L** ($C = 4*10^{-5}$ mol L^{-1}) (open gray circles). Respective Gaussian decompositions (dashed lines) and best fit (full black line) ($R = 0.99957$); (**b**) Theoretical absorption spectra of **H_2L** (black line). The sticks represent the mean contributions of the absorption spectra.

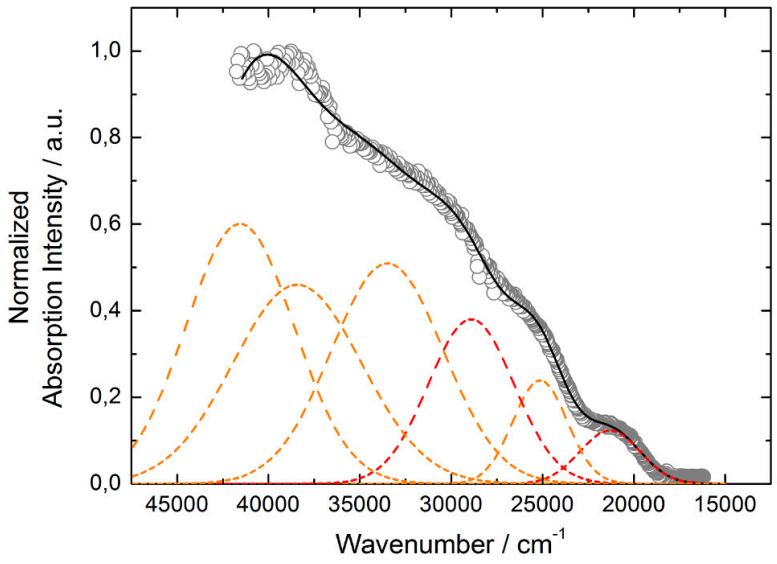

Figure S3. Experimental solid-state UV-VIS absorption spectrum (open circles) for **H_2L** at room temperature with respective Gaussian decompositions (dashed coloured lines) and best fit (full black line) R = 0.99814.

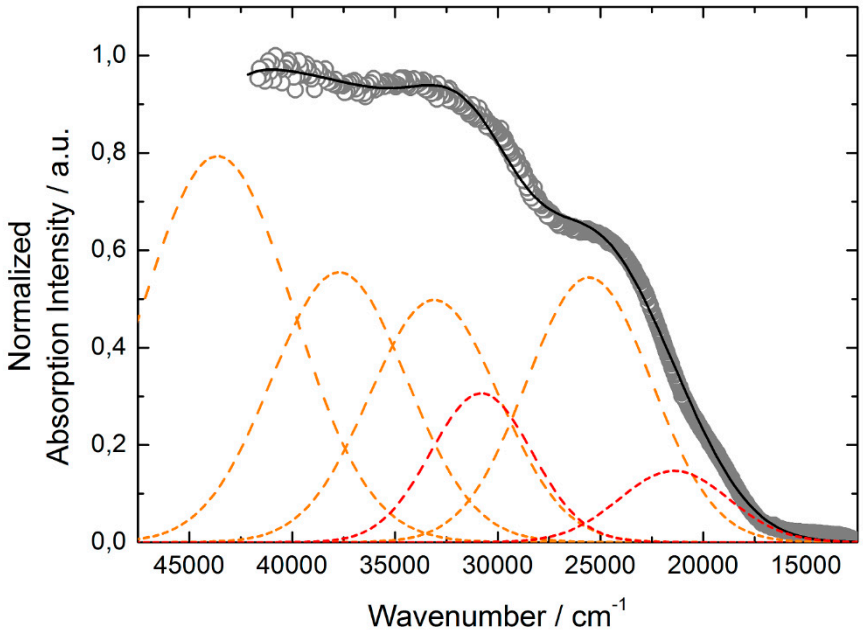

Figure S4. Experimental solid-state UV-VIS absorption spectrum (open circles) for **Na_2L** at room temperature with respective Gaussian decompositions (dashed coloured lines) and best fit (full black line) R = 0.99893.

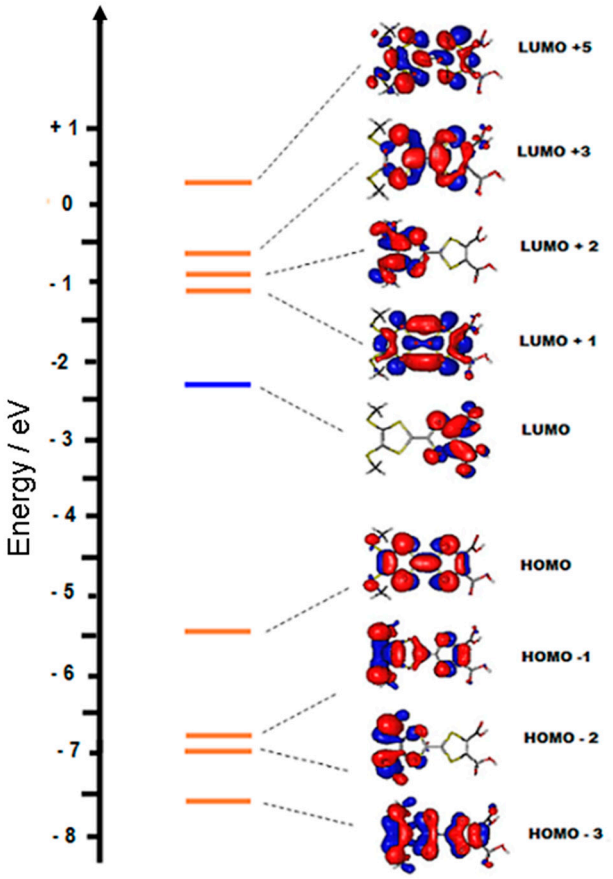

Figure S5. MO diagram of **H2L**. Energy levels of the centered TTF donor and carboxylic acceptor are represented in orange and blue, respectively.

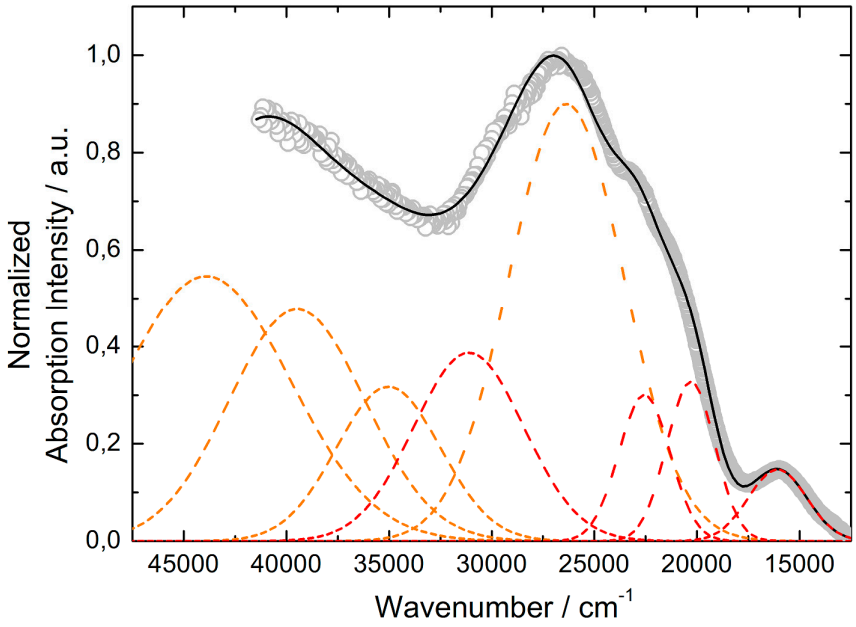

Figure S6. Experimental solid-state UV-VIS absorption spectrum (open circles) for **Yb** at room temperature with respective Gaussian decompositions (dashed coloured lines) and best fit (full black line) R = 0.99875.

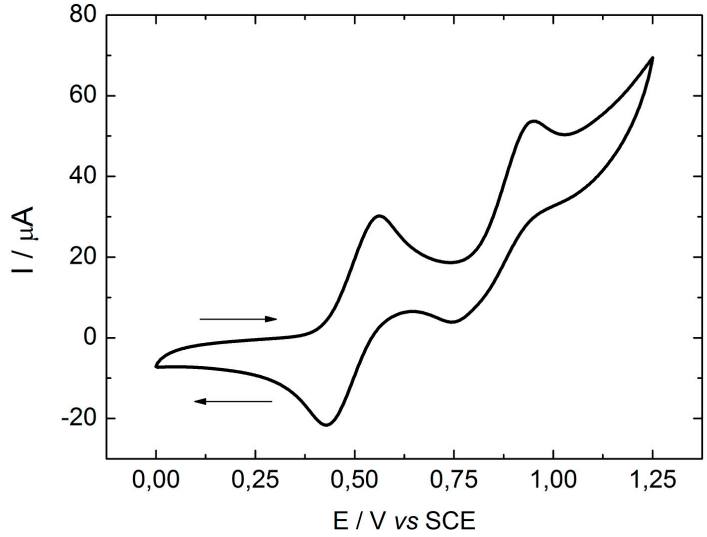

Figure S7. Cyclic voltametry of **Yb** in CH_2Cl_2 at a scan rate of 100 $mV.s^{-1}$.The potentials were measured *versus* a saturated calomel electrode (SCE); glassy carbon as the working electrode; Pt wire as the counter electrodes.

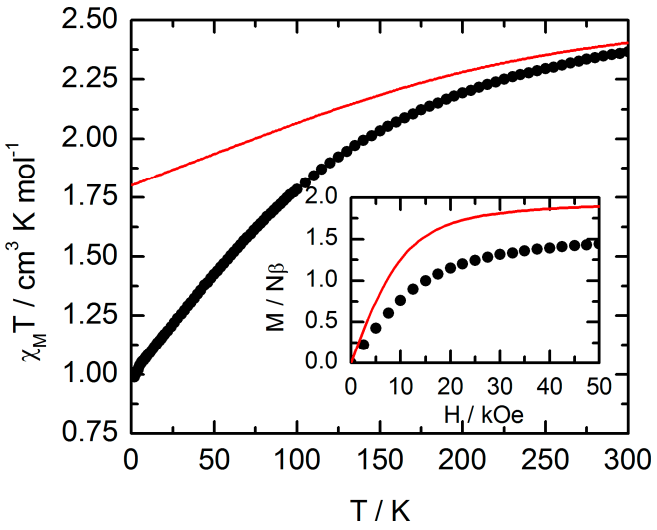

Figure S8. Temperature dependence of $\chi_M T$ for **Yb.** Inset: magnetic field dependence of the magnetization for **Yb** recorded at 2 K. Full red lines correspond to the *ab initio* simulated curves.

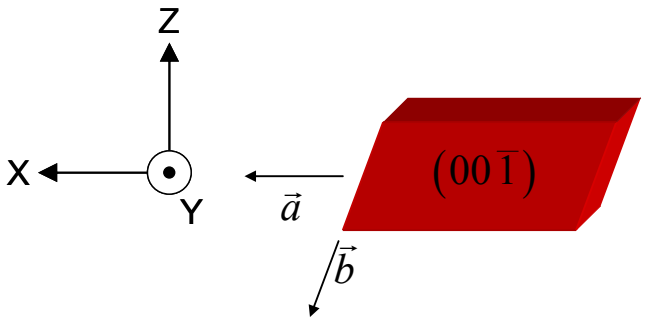

Figure S9. Oriented single crystal of **Yb** with the XYZ crystal reference frame.

Extended Debye Model

$$\chi_M' = \chi_S + (\chi_T - \chi_S)\frac{1+(\omega\tau)^{1-\alpha}\sin\left(\alpha\frac{\pi}{2}\right)}{1+2(\omega\tau)^{1-\alpha}\sin\left(\alpha\frac{\pi}{2}\right)+(\omega\tau)^{2-2\alpha}}$$
$$\chi_M'' = (\chi_T - \chi_S)\frac{(\omega\tau)^{1-\alpha}\cos\left(\alpha\frac{\pi}{2}\right)}{1+2(\omega\tau)^{1-\alpha}\sin\left(\alpha\frac{\pi}{2}\right)+(\omega\tau)^{2-2\alpha}} \quad (1)$$

Where χ_T is the isothermal susceptibility, χ_S the adiabatic susceptibility, τ the relaxation time and α an empiric parameter which describe the distribution of the relaxation time. For SMM with only one relaxing object α is close to zero. The extended Debye model was applied to fit simultaneously the experimental variations of χ_M' and χ_M'' with the frequency f of the oscillating field ($\omega = 2\pi f$). Typically, only the temperatures for which a maximum on the χ'' *vs.* f curves, have been considered. The best fitted parameters τ, α, χ_T, and χ_S are listed in Table S4 with the coefficient of determination R^2.

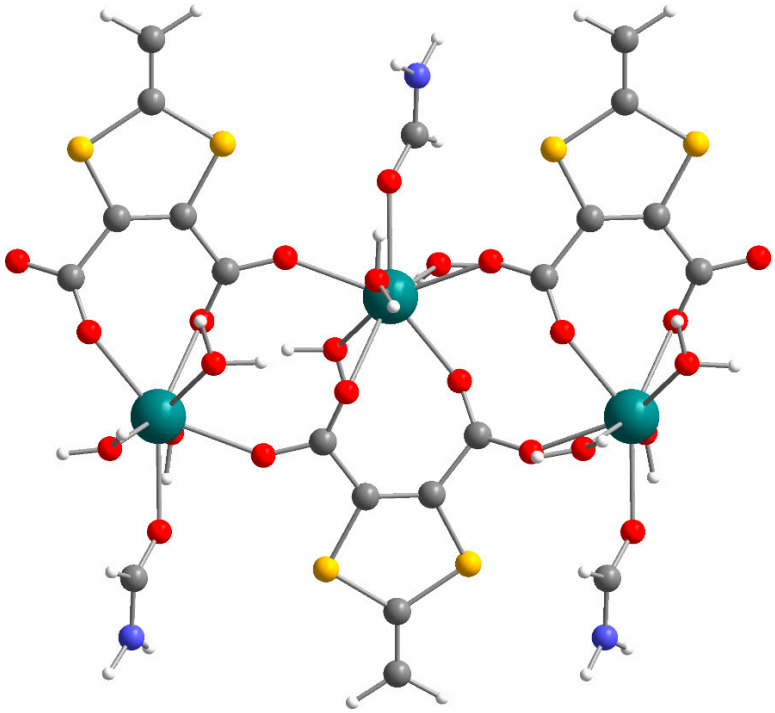

Figure S10. Model used in the CASSCF/PT2/SI-SO calculations. Oxygen atoms are in red, nitrogen in blue, carbon in grey, sulphur in yellow, and hydrogen in white.

Table S1. X-ray crystallographic data of **Yb**.

Compounds	Yb
Formula	$C_{23}H_{22}Yb_1N_1O_{13}S_{12}$
M / g.mol^{-1}	1077.0
Crystal system	Triclinic
Space group	P-1 (N°2)
Cell parameters	a = 7.8511(12) Å b = 9.7170(20) Å c = 25.4530(50) Å α = 89.631(9 ° β = 83.529(6) ° γ = 75.734(6) °
Volume / Å^3	1869.5(6)
Z	2
T / K	150 (2)
2θ range /°	1.62 ≤ 2θ ≤ 55.26
ρ_{calc} / g.cm^{-3}	1.912
μ / mm^{-1}	3.225
Independent reflections	10145
$Fo^2 > 2\sigma(Fo)^2$	9170
Number of variables	321
R_1, wR_2	0.0601, 0.1663

Table S2. TD-DFT calculated excitation energies and main compositions of the low-lying electronic transitions for **H_2L**. In addition, the charge transfers and the pure intramolecular transitions are reported. ID and H, L represent the intramolecular TTF (donor), the HOMO, and the LUMO, respectively. ILCT corresponds to intra-ligand charge transfer. The theoretical values are evaluated at the PCM(CH_3OH)-PBE0/SVP level of approximation.

	Energy exp (cm^{-1})	Energy theo (cm^{-1})	Osc.	Type	Assignment	Transition
H_2L	21,900	18,890	0.03	ILCT	$\pi_{TTF}\rightarrow\pi^*_{COOH}$	H→L (98%)
	27,100	29,535	0.04	ID	$\pi_{TTF}\rightarrow\pi^*_{TTF}$	H→L+2 (96%)
	31,100	31,034	0.02	ILCT	$\pi_{TTF}\rightarrow\pi^*_{COOH}$	H-1→L(95%)
		33,414	0.24	ID	$\pi_{TTF}\rightarrow\pi^*_{TTF}$	H→L+3 (66%)
	32,700	35,242	0.07			H→L+4 (74%)
		36,199	0.21			H→L+1/+5 (38/30%)
	38,200	40,712	0.10	ID	$\pi_{TTF}\rightarrow\pi^*_{TTF}$	H-2→L+1 (43%) H-1→L+2 (24%)
	44,100	44,510	0.15	ID	$\pi_{TTF}\rightarrow\pi^*_{TTF}$	H-3→L+1 (63%)

Table S3. Solid-state absorption data for ligands **H_2L, Na_2L**, and the coordination complex **Yb**.

Energy exp (cm^{-1}) for H_2L	Energy exp (cm^{-1}) for Na_2L	Energy exp (cm^{-1}) for Yb	Type
/	/	16,100	ILCT
21,300	/	20,300	ILCT
/	21,400	22,600	ILCT
25,100	25,600	26,364	ID
28,900	30,800	31,100	ILCT
33,500	33,100	35,000	ID
38,400	37,700	39,500	ID
41,600	43,600	43,900	ID

Table S4. Best fitted parameters (χ_T, χ_S, τ, and α) with the extended Debye model **Yb** at 1 kOe in the temperature range 1.8-5 K.

T / K	χ_T / cm^3 mol^{-1}	χ_S / cm^3 mol^{-1}	α	τ / s	R^2
1.8	0.5648	0.10449	0.35242	0.00121	0.99954
2	0.51898	0.09579	0.35963	0.00101	0.99964
2.2	0.47729	0.09722	0.3424	9.21×10^{-04}	0.99973
2.4	0.43639	0.08982	0.33651	7.69×10^{-04}	0.99942
2.6	0.40376	0.08314	0.32612	6.50×10^{-04}	0.99951
2.8	0.37438	0.08662	0.29506	5.94×10^{-04}	0.99948
3	0.35051	0.0823	0.28158	4.91×10^{-04}	0.99949
3.5	0.30013	0.08357	0.19534	3.22×10^{-04}	0.99967
4	0.26275	0.08062	0.1158	1.88×10^{-04}	0.99981
4.5	0.23458	0.08072	0.02866	1.15×10^{-04}	0.99987
5	0.21182	0.07543	7.70×10^{-04}	6.60×10^{-05}	0.99996